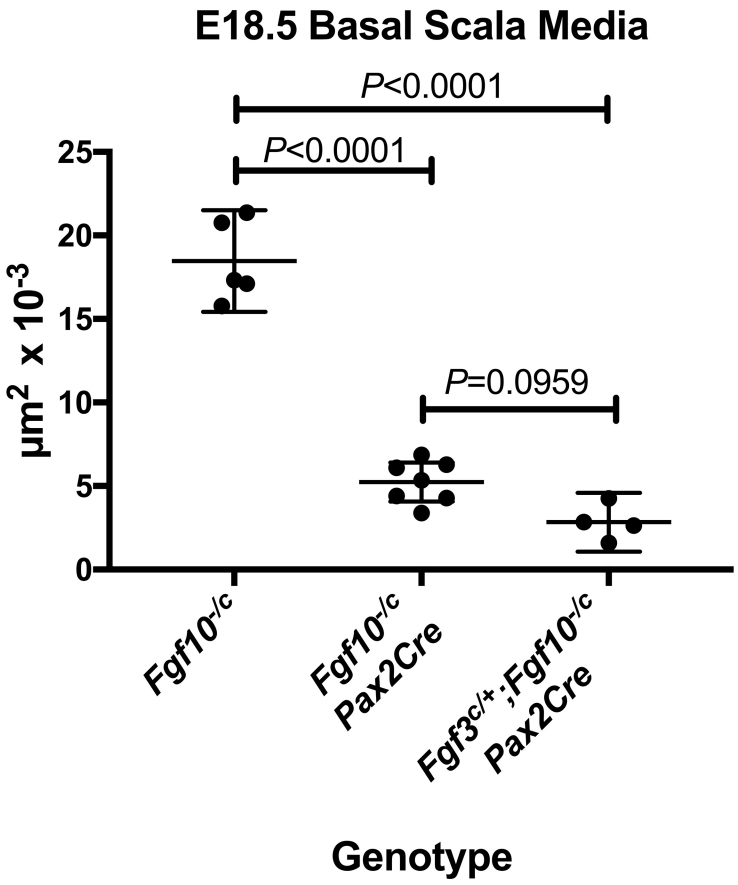

Figure S1. Removing one copy of *Fgf3* from the F10cKO background does not significantly affect the area of the scala media. Scala media area (μm^2) was determined for three genotypes, *Fgf10*$^{-/c}$ (controls, n=5, not shown in Fig. 2), *Fgf10*$^{-/c}$*;Pax2-Cre/+* (F10CKO, n=6; Fig. 2G) and *Fgf3*$^{c/+}$*;Fgf10*$^{c/-}$*;Pax2-Cre/+* (F3cHet;F10CKO, n=4; Fig. 2R). Mean and 95% confidence intervals are indicated. One-way ANOVA with Tukey's multiple comparisons test was used to calculate significance.

Development • Supplementary information

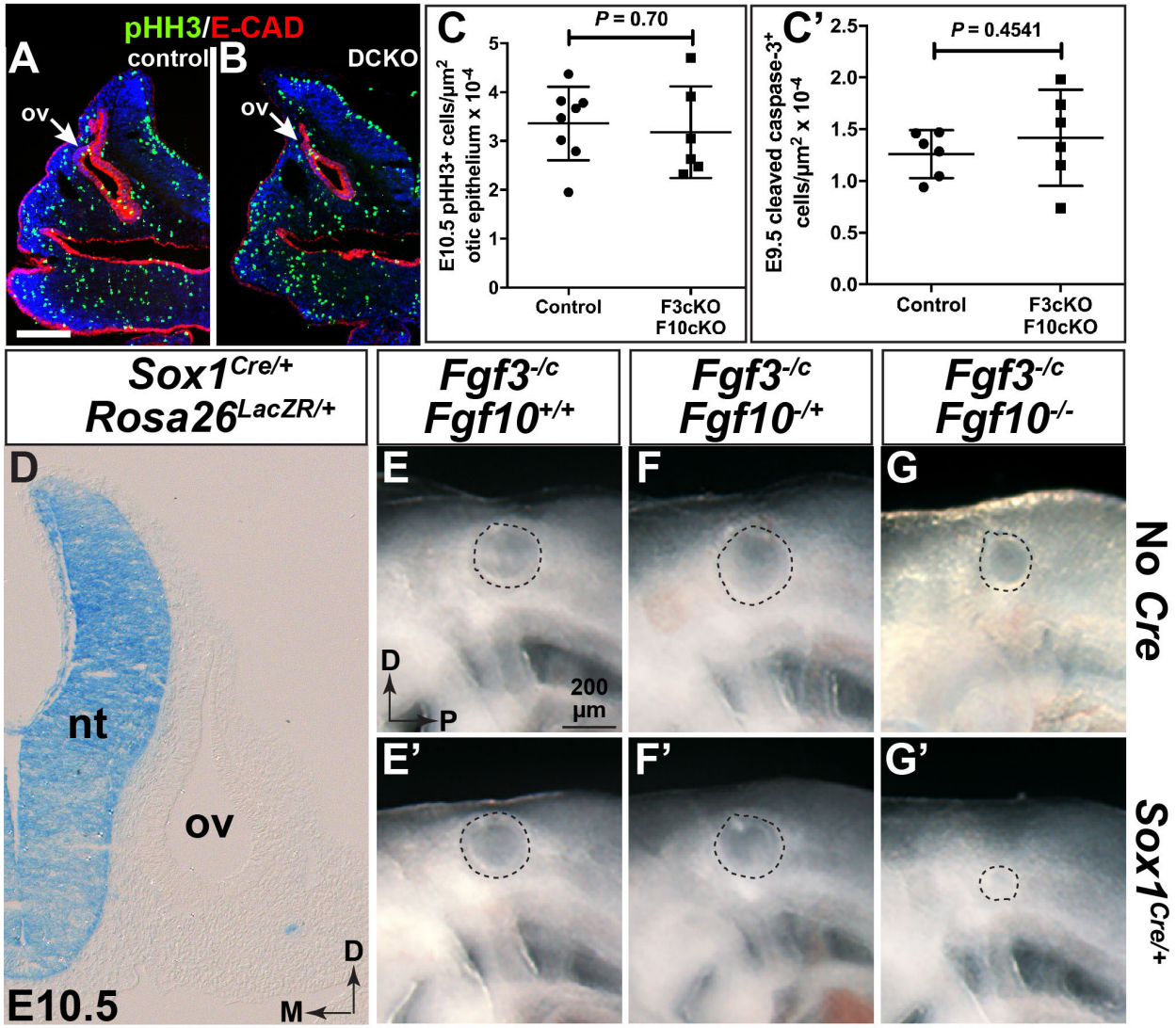

Figure S2. *Fgf3* and *Fgf10* are not required in the *Pax2-Cre* lineage for early otocyst proliferation or survival, likely because *Fgf3* expression persists in the hindbrain, where it is required for development of a normally sized otic vesicle. (A,B) Transverse cryosections of E10.5 control (*Fgf3*$^{-/c}$;*Fgf10*$^{-/c}$) and double conditional mutant (DCKO; *Fgf3*$^{-/c}$;*Fgf10*$^{-/c}$;Tg(*Pax2-Cre*)/+) otic vesicles (ov) immunostained to detect pHH3 (green) and E-Cadherin (red). Scale bar in A (100 µm) applies to B. (C) Quantification of pHH3-positive cells per otic epithelial area shows no significant difference between genotypes. (C') Quantification of cleaved-caspase-3 cells per otic epithelial area shows no significant difference between genotypes at E9.5. (D) Transverse section at the level of the otic vesicle of an E10.5 X-gal-stained *Rosa26*$^{LacZR/+}$;*Sox1*$^{Cre/+}$ embryo shows CRE activity restricted to the neural tube. (E-G') Lateral views of otic vesicles from freshly dissected E9.5 embryos show that in the global absence of *Fgf10*, hindbrain *Fgf3* is required to develop a normally sized otic vesicle (G'). *Fgf* genotypes are indicated above and *Cre* status is to the right of each row. Dashed lines denote the external circumference of the otic epithelium. The scale bar and orientation axes in E apply to E-G'. Abbreviations: D, dorsal; M, medial, nt, neural tube; ov, otic vesicle; P, posterior.

Development • Supplementary information

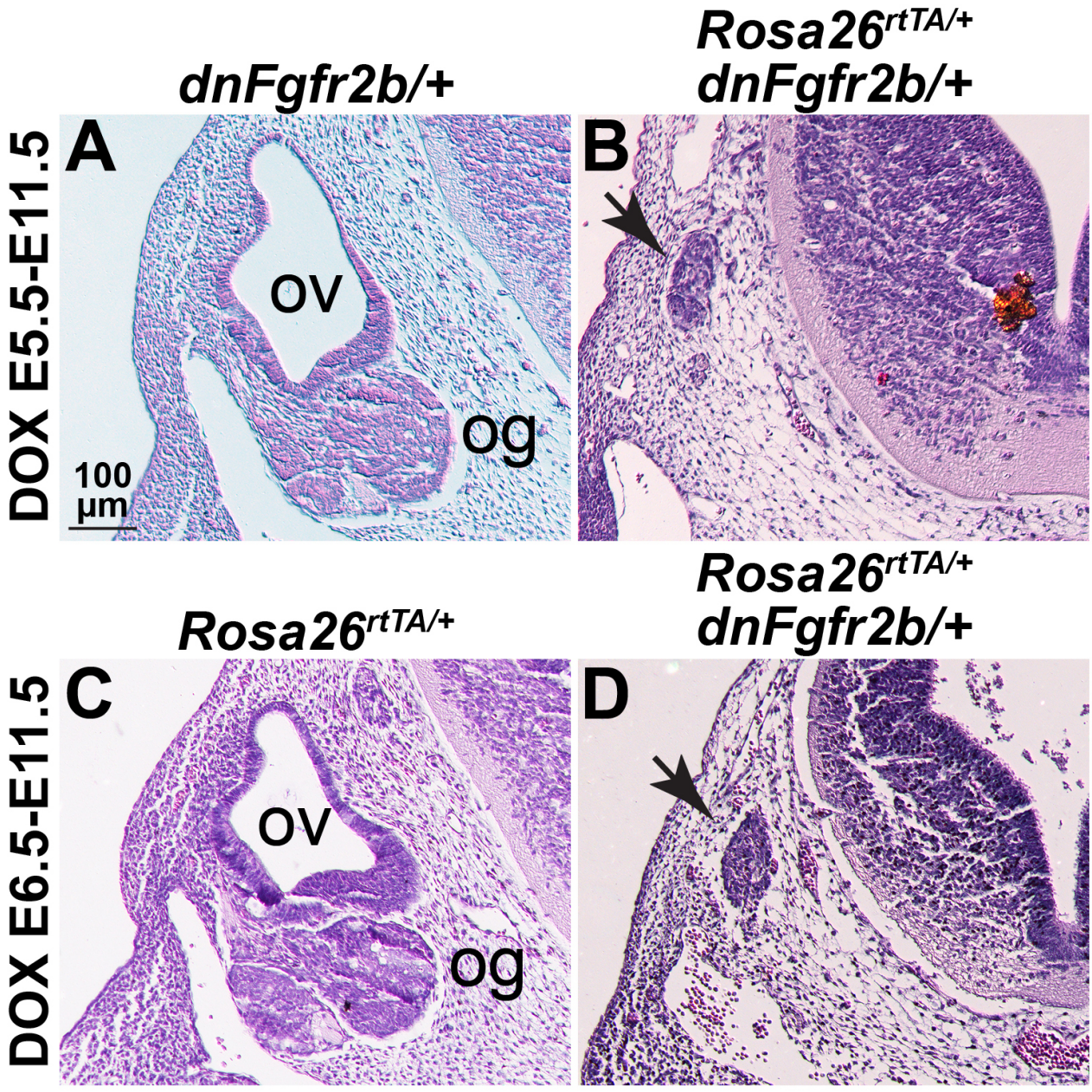

Figure S3. Induction of dnFGFR2b prior to otic placode induction blocks otic vesicle formation. Transverse hematoxylin and eosin-stained sections of embryos derived from Tg(*tetO-dnFgfr2b*)/+ females crossed to *Rosa26*$^{rtTA/+}$ males and fed DOX-chow between E5.5-E11.5 (A,B) or E6.5-E11.5 (C,D). Genotypes are indicated above each column and DOX induction conditions indicated to the left of each row. Remnant otic tissue in the experimental samples is indicated with an arrow (B,D). The scale bar in A applies to all panels. Abbreviations: og, otic ganglion; ov, otic vesicle.

Development • Supplementary information

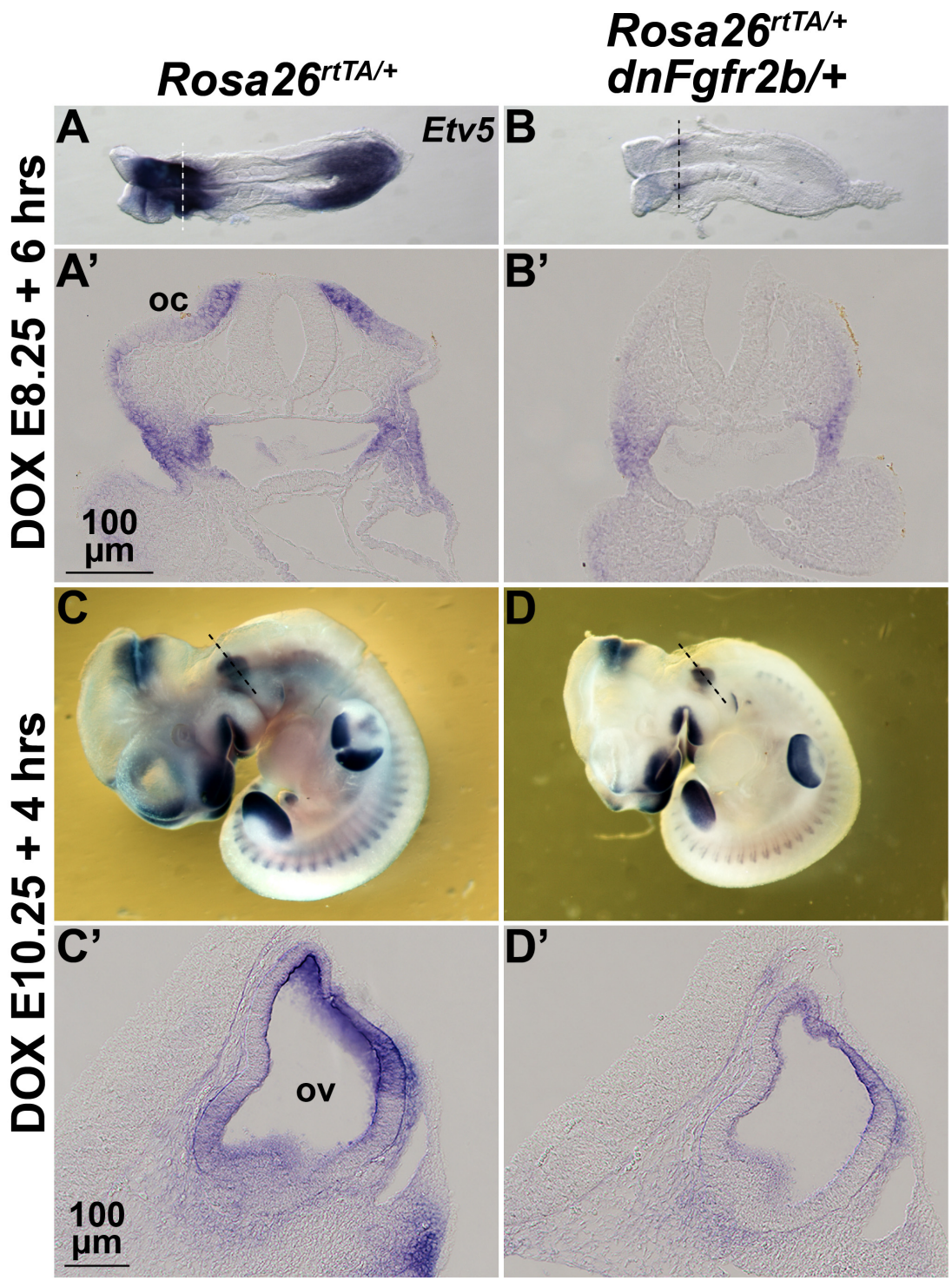

Figure S4. Inhibition of FGFR2b ligands has a rapid onset. Whole-mount ISH with an *Etv5* probe on embryos derived from wild type females crossed to *Rosa26*$^{rtTA/rtTA}$;Tg(*tetO-dnFgfr2b*)/+ males and treated with DOX for six hours beginning at E8.25 (A-B') or 4 hours beginning at E10.5 (C-D'). Genotypes are indicated above each column. Dashed lines (A,B,C,D) indicate the planes of transverse sections shown in A',B',C',D'. Abbreviations: oc, otic cup; ov, otic vesicle.

Development • Supplementary information

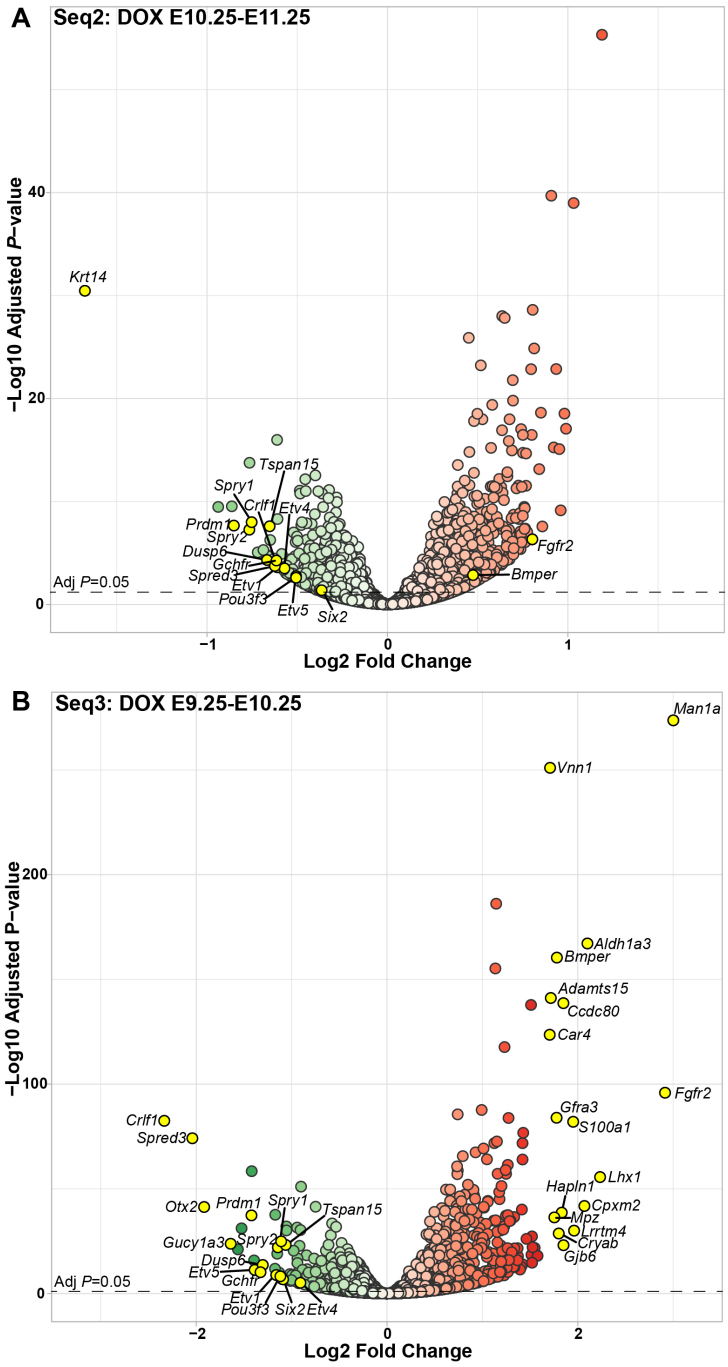

Figure S5. Differential RNA-Seq analysis of otic epithelia subjected to overlapping and longer dnFGFR2b induction windows define a stage-specific FGFR2b signaling response during early otic morphogenesis. (A) Volcano plot of the RNA-Seq2 (DOX exposure E10.25-E11.25), and (B) RNA-Seq3 (DOX exposure from E9.25-E10.25) datasets. Down-regulated (green) and up-regulated (red) genes were identified using a paired statistical model (see Methods). The statistical significance of the differential expression is shown on the y-axis and the fold change is shown on the x-axis. Names for genes highlighted in yellow include all those with a fold-change > 1.5, plus known FGF target genes and genes that we pursued for expression validation.

Development • Supplementary information

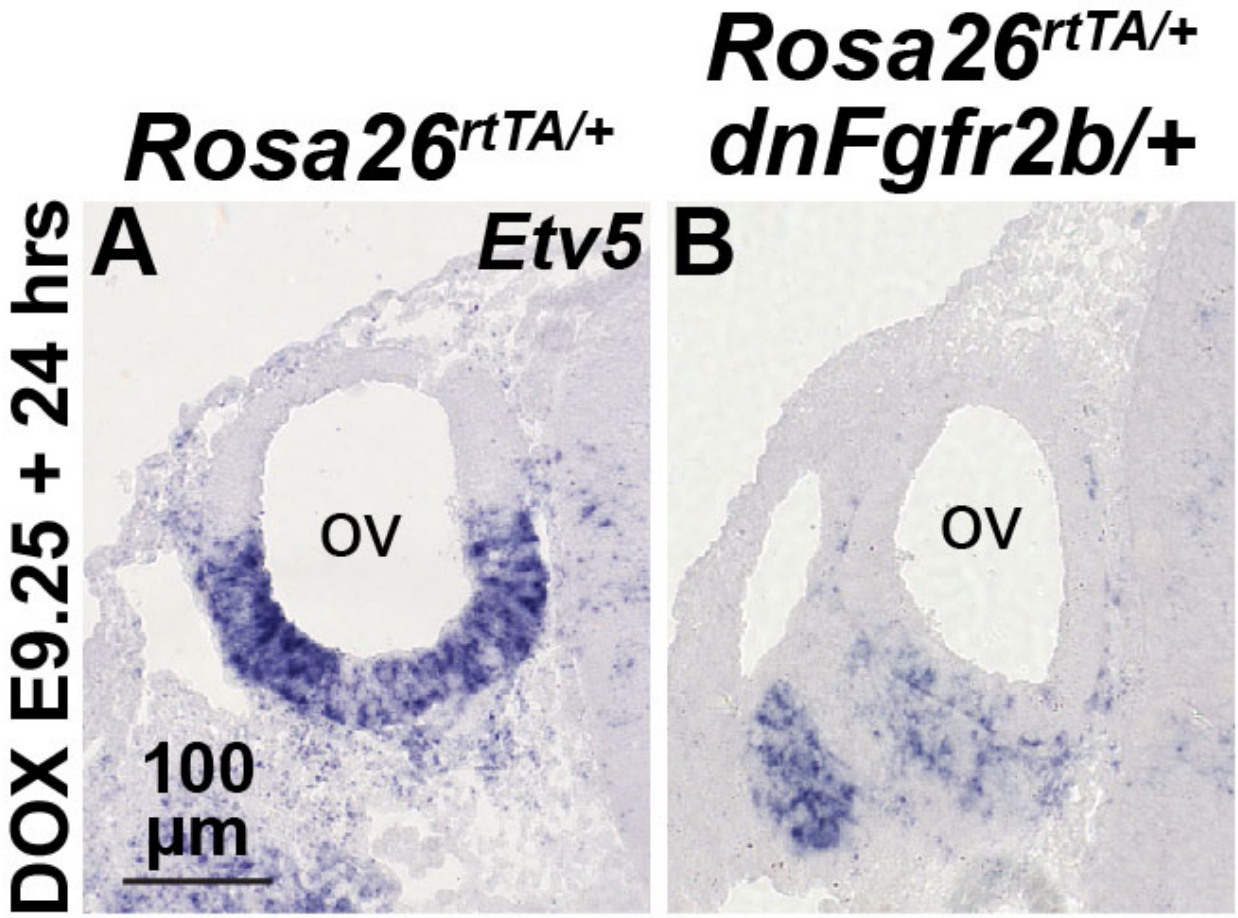

Figure S6. *Etv5* is lost from the otic vesicle following RNA-Seq3 dnFGFR2b induction conditions. ISH using an *Etv5* probe on sections taken through the otic vesicle (ov) and ganglion (og) from control (A) (*Rosa26*$^{rtTA/+}$) or *dnFgfr2b*-expressing embryos (B) subjected to Seq3 induction conditions (E9.25-E10.25, n=3 each).

Development • Supplementary information

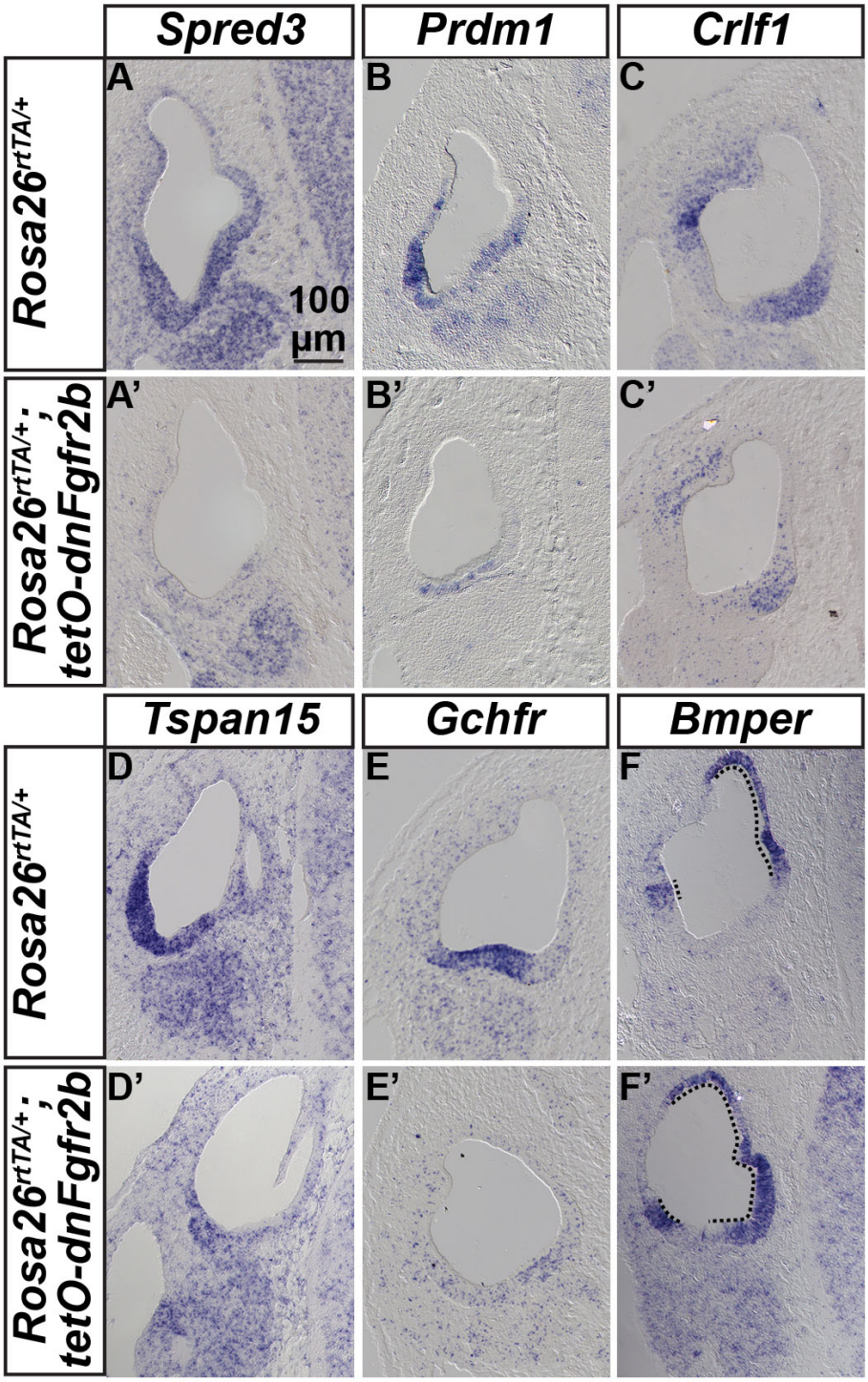

Figure S7. Validation of the subset of new FGFR2b ligand-dependent genes differentially expressed under RNA-Seq2 induction conditions. ISH of transverse E11.25 paraffin sections of otocysts exposed to Seq2 induction conditions (DOX, E10.25-E11.25). Probes are indicated in the boxes above each column and genotypes are indicated to the left of each row (controls A-F, dnFGFR2b-expressing embryos A'-F', n=3 each). Dorsal is up, medial is to the right. The scale bar in A applies to all panels. The dotted line in F and F' demarks *Bmper* expression.

Development • Supplementary information

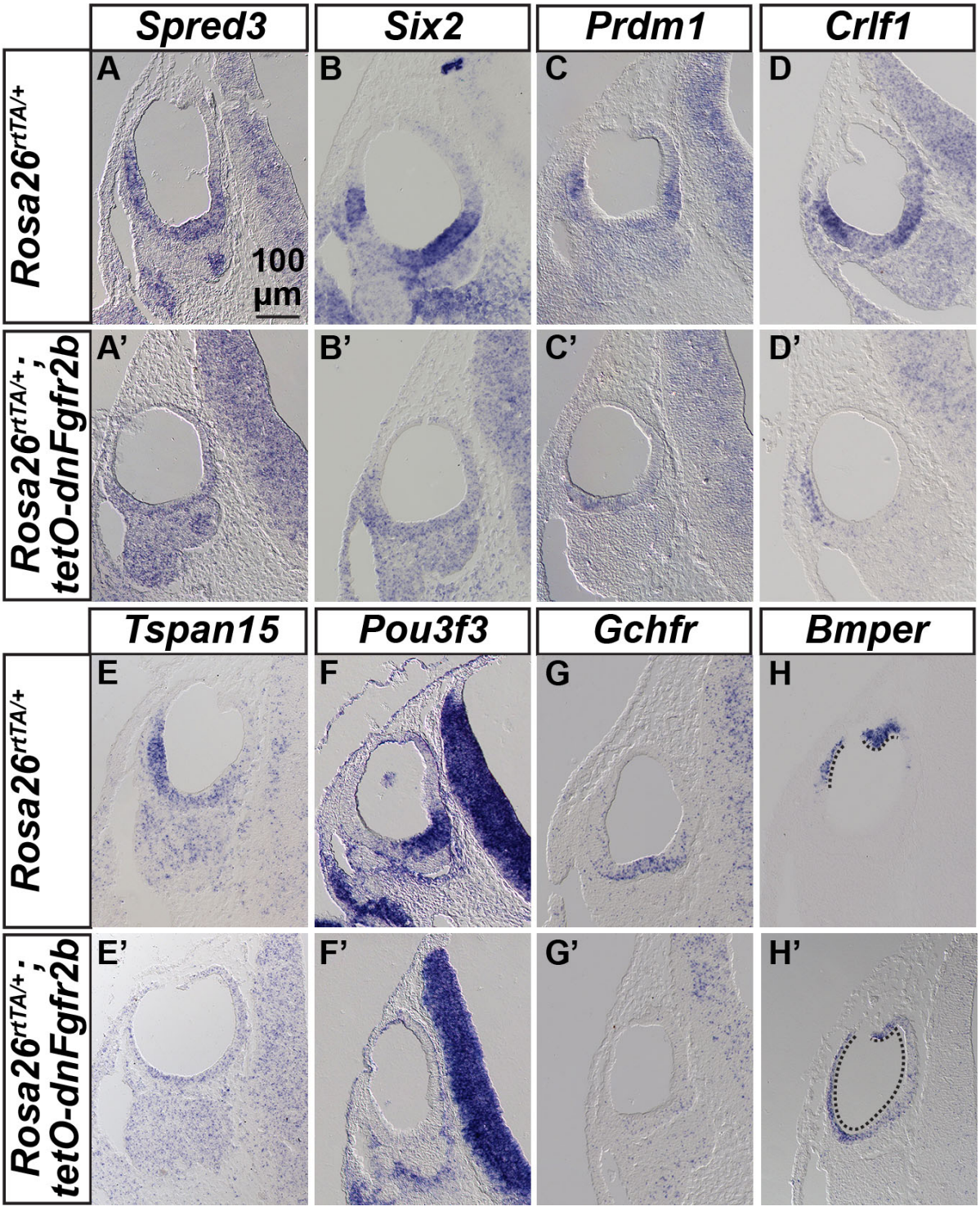

Figure S8. Validation of the subset of new FGFR2b ligand-dependent genes differentially expressed under RNA-Seq3 induction conditions. ISH of transverse E10.25 paraffin sections of otocysts exposed to Seq3 induction conditions (DOX, E9.25-E10.25). Probes are indicated in the boxes above each column and genotypes are indicated to the left of each row (controls A-H, dnFGFR2b-expressing embryos A'-H', n=3 each). Dorsal is up, medial is to the right. The scale bar in A applies to all panels. The dotted line in H and H' demarks *Bmper* expression.

Development • Supplementary information

Table S1

Phenotypes resulting from loss of epithelial *Fgf3* and *Fgf10* alleles in the Tg(*Pax2-Cre*) lineage

CRE negative	*Fgf3*$^{-/c}$	*Fgf10*$^{-/c}$	*Fgf3*$^{c/+}$; *Fgf10*$^{c/+}$	*Fgf3*$^{-/c}$; *Fgf10*$^{c/+}$	*Fgf3*$^{c/+}$; *Fgf10*$^{-/c}$	*Fgf3*$^{-/c}$; *Fgf10*$^{-/c}$
C0	**4**	0	**10**	3	0	0
C1	0	**4**	1	**9**	6	0
C2	0	3	0	0	**6**	**6**
C3	0	0	0	0	2	0
C4	0	0	0	0	0	0
C5	0	0	0	0	0	0

CRE positive	*Fgf3*$^{-/c}$	*Fgf10*$^{-/c}$	*Fgf3*$^{c/+}$; *Fgf10*$^{c/+}$	*Fgf3*$^{-/c}$; *Fgf10*$^{c/+}$	*Fgf3*$^{c/+}$; *Fgf10*$^{-/c}$	*Fgf3*$^{-/c}$; *Fgf10*$^{-/c}$
C0	**8**	0	0	0	0	0
C1	0	2	**9**	3	0	0
C2	0	**8**	3	**11**	0	0
C3	0	6	0	0	2	0
C4	0	0	0	0	**13**	0
C5	0	0	0	0	2	**16**

Gross phenotypic classes
C0=normal morphology
C1=reduced PSCC, normal cochlea
C2=absent PSCC, normal cochlea
C3=absent PSCC/variable lscc and ascc, short cochlea
C4=unfused vertical canal pouches, shortened cochlea
C5=spheroid chamber lacking distinct vestibule or cochlea

Scoring of paintfill phenotypic classes by *Fgf* genotype and *Pax2-Cre* status. C0-C4 were defined previously by Urness et al. (2015) for *Fgf10* heterozygous and homozygous germline mutants. C5, the most severe class, was never observed in *Fgf10* germline mutants. The most prevalent phenotype for each genotype is indicated in bold; examples of the most prevalent phenotypes are shown in Figure 2L-O'. The distribution of phenotypes is significantly different between the F10cKO and F3cHet;F10cKO ears (P<0.0001; Fisher's exact test; SPSS software).

Development • Supplementary information

Table S2

cDNA clones used to prepare digoxigenin-labeled cRNA antisense transcripts for in situ hybridization

Gene	Insert size (bp)	Enzyme (antisense)	Poly-merase	Source	Reference
Bmp4	~900	AccI	T7	Anne Boulet	Jones et al., 1991
Sox9	~400	EcoRI	T3	Anne Boulet	Wright et al., 1995
Fgf3	373	BamHI	T3	Nancy Manley	Wright and Mansour, 2003
Fgf10	~550	EcoRI	SP6	David Ornitz	Xu et al., 1998
Etv5	458	EcoRI	T7	GenBank NM_023794 Residues 1309-1766	Li et al., 2007
Gbx2	~1000	HindIII	T7	Gail Martin	Wassarman et al., 1997
Sox2	530	HindIII	T7	Olivia Bermingham-McDonogh	Wood and Episkopou, 1999
Foxg1	~400	HindIII	T7	GenBank A1592649 Residues 2615-2976	Pauley et al., 2006
Pax2	~500	BamHI	T3	Peter Gruss	Dressler et al., 1990
Neurod1	~1500	EcoRI	T3	Gary Gaufo	Liu et al., 2000
Neurog1	~2000 (hydrolyzed)	XhoI	T7	Quifu Ma	Ma et al., 2000

Purified plasmid DNA was digested with the indicated restriction enzyme and then transcribed with the indicated RNA polymerase to produce antisense probes for ISH.

Development • Supplementary information

Table S3

Primers used to generate DNA fragments for cRNA probe generation.

Gene	Primers	Primer sequences (5'-3')	Product size (bp)
Spred3	F-916	TTCTACCGTTCACTGGGATTCC	~675
	R-915	CCAAACCAGCTCAACAATCC	
Six2	F-936	AGTTCCGAGGATGAGAAGACG	~510
	R-937	CTTGCCTAGTTCAAGACTCGG	
Prdm1	F-908	ATCCATCTCTGCAGCCTCAAGG	~490
	R-907	GCAGATCTGGAGTCATGTACAAGC	
Tspan15	F-968	TACTGTACATCACCCGTGTGG	~625
	R-969	AGCCTTACAGAGGACTCAAGG	
Pou3f3	F-925	GGGACATCTCGTTTATACTGTGG	~745
	R-926	TGTCTTTCCACACCCTTTTATCGG	
Gchfr	F-939	ACGAATACTACGTCAACGACC	~460
	R-940	GAACAACCACTTGTGAGAGCC	
Bmper	F-970	GTGATAACTGGAATGAGATCGG	~670
	R-971	GTGAAATCTGACAGACTCTCCTTGG	
*Crlf1**	F-946	AGCAGTCAGGAGACAATCTGG	~620
	R-947	AACGCACTTGGACAAGTAAACGG	

Forward (F) and reverse (R) primers used to PCR-amplify 3'UTR regions of each indicated gene from mouse genomic DNA, except *Crlf1*, which was amplified from a cDNA clone. All reverse primers include the T7 promoter sequence (GGATCCTAATACGACTCACTATAGGGAG) at the 5' end. The antisense-RNA strand was produced by transcription of the PCR product using T7 RNA polymerase. *Crlf1* cDNA 3 from DNASU Arizona State University Clone # MmCD00295268 (NCBI NM_018827.2, Image: 100063851).

Development • Supplementary information

Table S4.

Sheet 1: Fgfs, Fgfrs, targets
Compilation of normalized mean control and experimental count values from DSeq2 paired analyses for *Fgfs*, *Fgfrs* and select target genes with corresponding log2FoldChange and adjusted *P*-values (padj) from the RNA-Seq1, -Seq2 and -Seq3 datasets. Ensembl mouse gene numbers are shown (col A) if the gene was detected in at least one of the datasets. Gene names (col B) follow mouse conventions. Log2FoldChange cells are shaded in red to indicate significant upregulation and in green to indicate significant downregulation, roughly corresponding to the scheme used in the volcano plots. Padj values were derived following the Benjamini-Hochberg multiple testing correction. NA in the padj column indicates that there were outlier counts present in one or more groups.

Sheet 2: IPA,GO_paired top 5 path
Output of Ingenuity Pathway and GOrilla analyses. Rows 3-21 Ingenuity Pathway Analysis (IPA) output for the top 5 regulated pathways in each RNA-seq dataset. The cutoff for differential expression P-value in each dataset was 0.05. There was no cutoff for fold-change. Column heading definitions are shown on the sheet. Rows 35-61. GOrilla process analysis output for downregulated genes with an adjusted P-value of <0.05 and no fold-change cutoff in RNA-Seq1-3 paired datasets and GOrilla function analysis for downregulated genes in RNA-Seq1 with a Max AdjP-value <0.05 and log2(fold-change) >0.585. (http://cbl-gorilla.cs.technion.ac.il/) Column heading definitions are shown on the sheet.

Sheet 3: Seq1 GSEA_AORL,NISHIO
Gene set enrichment analysis (GSEA) of all 16232 RNA-Seq1 genes ranked by fold-change, using 93 human hearing loss genes listed in Nishio et al. (2015) (https://software.broadinstitute.org/gsea/doc/GSEAUserGuideFrame.html), including the enrichment table (cols A-H) and plot. GSEA column heading and plot definitions are shown on the sheet.

Sheet 4: Seq1 GSEA_JAX
Gene set enrichment analysis (GSEA) of all 16232 RNA-Seq1 genes ranked by fold-change, using 258 mouse inner ear-associated genes listed in Ohlemiller et al. (2016) (https://software.broadinstitute.org/gsea/doc/GSEAUserGuideFrame.html) including the enrichment table (cols A-H) and plot. GSEA column heading and plot definitions are shown on the sheet.

Sheet 5: intersect datasets
Intersections of downregulated and upregulated RNA-Seq1-3 gene lists with corresponding Venn diagrams generated using GeneVenn software (http://genevenn.sourceforge.net/). Downregulated genes with an AdjP <0.05 and FC>1.5 were overlapped separately from upregulated genes with an AdjP <0.01 and FC> 2. Gene lists comprising overlap in all three sets and for each pair are shown. Annotations of the gene lists are shown on the sheet.

Click here to Download Table S4

Development • Supplementary information